Bulletin of the Earthquake
Research Institute
Vol. 47 (1969), pp. 701-719

30. A Long Wave around a Breakwater [VII].
— Case of Normal Incidence —

By Takao Momoi,

Earthquake Research Institute.

(Read May 27, 1969.—Received May 30, 1969.)

Abstract

Succeeding the previous works, the long wave around the breakwater gap in the case of the normal incidence of the incident wave is further discussed in the present paper. The discussed problems are concerned with (1) the agreement of Blue-Johnson's theory with ours, (2) the effect of the breakwater terminus upon the diffracted wave, (3) the secondarily reflected wave and (4) the wave around a single breakwater wing. The agreement of Blue-Johnson's theory with ours is fairly good down to $kd=0.5$ (k: the wave number, d: half the width of the breakwater gap). For small kd, the strong emission of the secondary wave is found from the shadow of the breakwater. Through the numerical calculation of the wave around the single breakwater wing, it is inquired to what extent the resulting phenomena around the double breakwater wings come from the coupling effect of the two breakwaters.

1. Introduction

We have already discussed the long wave around the breakwater in seven papers with the same title (*Momoi*, 1967–1969). The present paper is a further contribution to the investigation into the long wave around the breakwater with an aperture.

2. Comparison with the Solution of Mirror Image

In 1949, Blue-Johnson devised an approximated theory on the wave around the breakwater wing with the gap for the case of normal incidence of a train of periodic waves (*Blue-Johnson*, 1949). Using their theory, Morihira and Okuyama computed the amplitude in the leeward waters for the parameter kd down to $\pi/2$. The comparison of our theory and Blue-Johnson's was made in the fifth work (*Momoi*, 1968c) by use of Morihira and Okuyama's result. The agreement is then found to be fairly good for kd down to $\pi/2$ at least. In the above, k and d are the wave number of the incident wave and half the width of the breakwater gap respectively. In Blue-Johnson's

work, they determined the application range of their approximated theory to be $b \gtrsim 2L$ (b and L: the breadth of the breakwater gap and the wave-length in their notation) using the asymptotic expression (refer to (12) of their paper). This estimation is considered to be slightly rough. With a view to assessing the applicable lower limit of their theory and inquiring to what extent the resulting amplitude and phase variations are in accord with those based on the author's rigorous theory which has been developed so far in the previous papers (*Momoi*, 1967a and 1967b), the further calculation of the wave by use of the approximated theory is carried out down to $kd=0.5$.

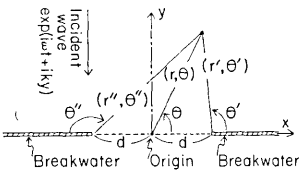

Fig. 1. Nomenclature of the model used.

The same approximated (mirror image) solution as that devised by Blue-Johnson is readily derived using the theory developed by Stoker for the case of a single breakwater (*Stoker*, 1957). The expression is as follows.

Let ζ^{mirror} be the wave height of the resultant wave for the model of the twin breakwaters (based on the method of mirror image), ζ^{right} and ζ^{left} those for the models of the right-hand and left-hand single breakwater wings (refer to Fig. 1).

$$\zeta^{mirror}=\zeta^{right}+\zeta^{left}-\exp(iky) \tag{1}$$

where

$$\left.\begin{aligned}\zeta^{right}&=J_0(kr')+2\sum_{n=1}^{\infty}e^{in\pi/4}J_{n/2}(kr')\cos\frac{n\pi}{4}\cos\frac{n\theta'}{2}\,,\\ \zeta^{left}&=J_0(kr'')+2\sum_{n=1}^{\infty}e^{in\pi/4}J_{n/2}(kr'')\cos\frac{n\pi}{4}\cos\frac{n\theta''}{2}\,,\end{aligned}\right\} \tag{2}$$

and the time factor is omitted as usual. For the definition and notation, the reader should refer to Fig. 1.

Using expression (1), the numerical calculation of the wave around the breakwater gap is carried out. The results are given in Figs. 2aw (pw, al, pl) to 6aw (pw, al, pl). Inspection of these figures reveals that the variations based on the method of mirror image is in fairly good agreement with those by the rigorous method (the method of the buffer domain) down to $kd=0.5$. According to Figs. 22*l* (*m*), 23*l* (*m*), 24 and 25 in the fifth work (*Momoi*, 1968c), Lamb's approximated theory is found to be well applicable for the discussion of the wave around the breakwater. The gross behaviors of the wave around the breakwater gap in the case of normal incidence of the incident wave are, therefore, discussed by use of two approximated theories, one of

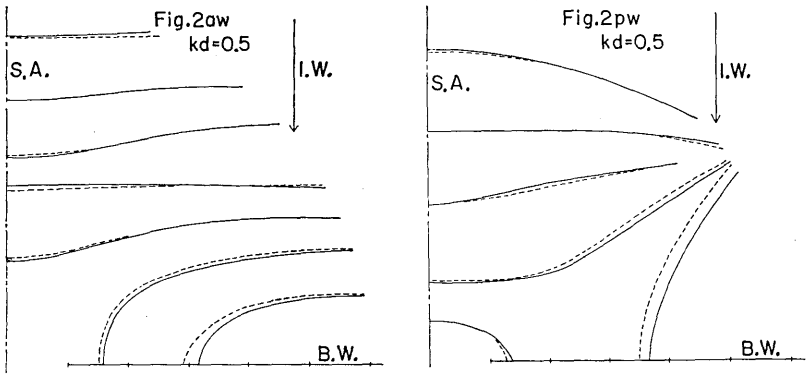

Fig. 2aw (pw). Comparison of the amplitudes (phases) in the windward based on the rigorous and mirror image method.*

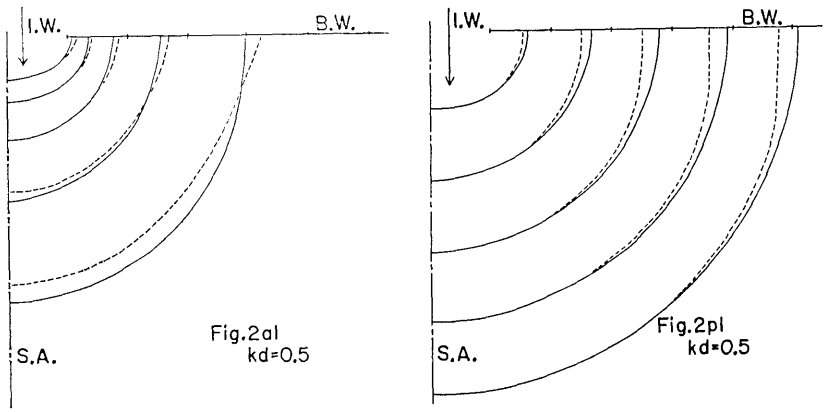

Fig. 2al (pl). Comparison of the amplitudes (phases) in the leeward based on the rigorous and mirror image method.*

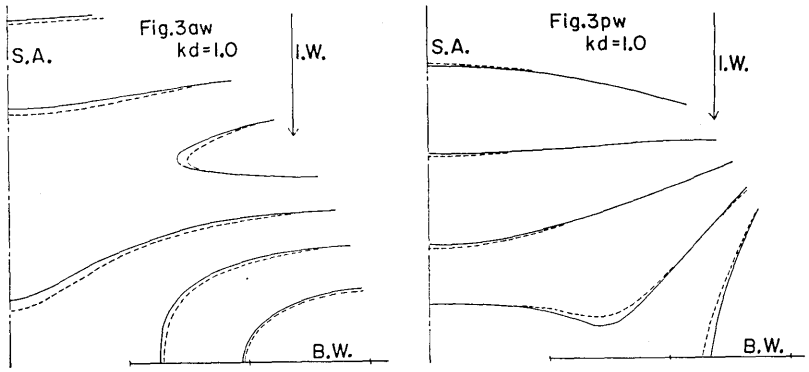

Fig. 3aw (pw). Comparison of the amplitudes (phases) in the windward based on the rigorous and mirror image method.*

* The solid and broken lines are the curves, respectively, based on the rigorous and mirror image method. **I. W., S. A.** and **B. W.** are the abbreviations of incident wave, symmetrical axis and breakwater.

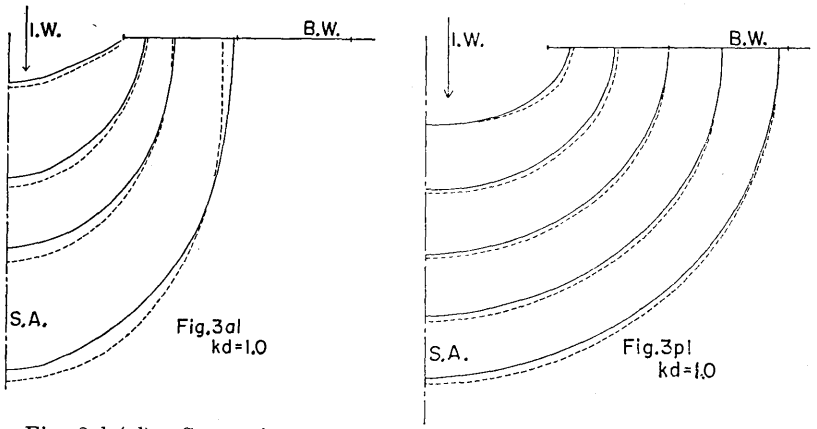

Fig. 3al (pl). Comparison of the amplitudes (phases) in the leeward based on the rigorous and mirror image method.*

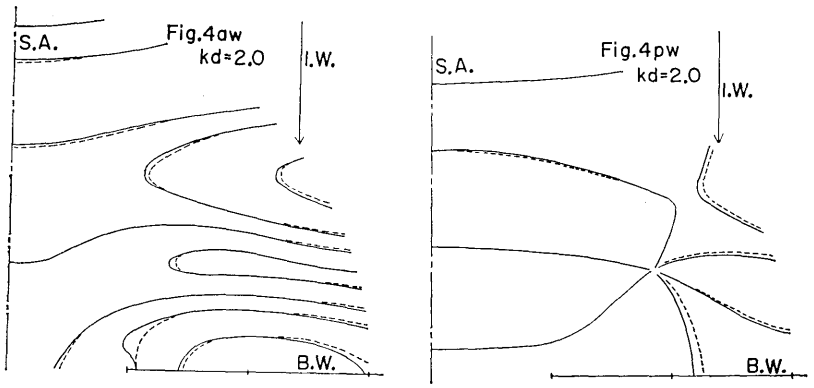

Fig. 4aw (pw). Comparison of the amplitudes (phases) in the windward based on the rigorous and mirror image method.*

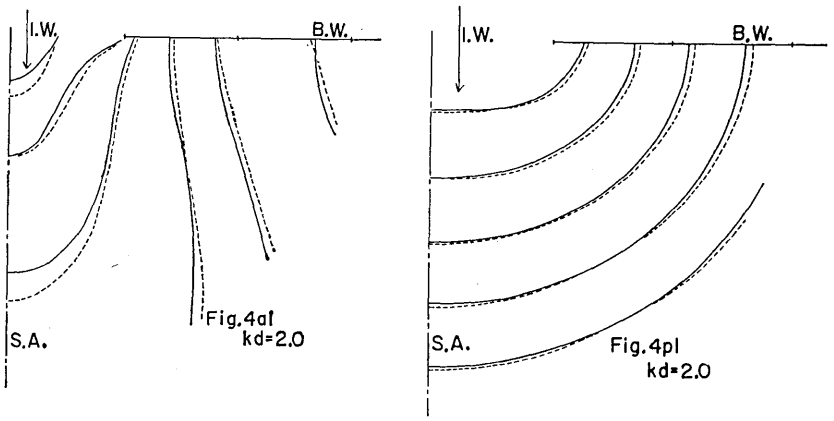

Fig. 4al (pl). Comparison of the amplitudes (phases) in the leeward based on the rigorous and mirror image method.*

* See the footnote of Figs. 2aw (pw)—3aw (pw).

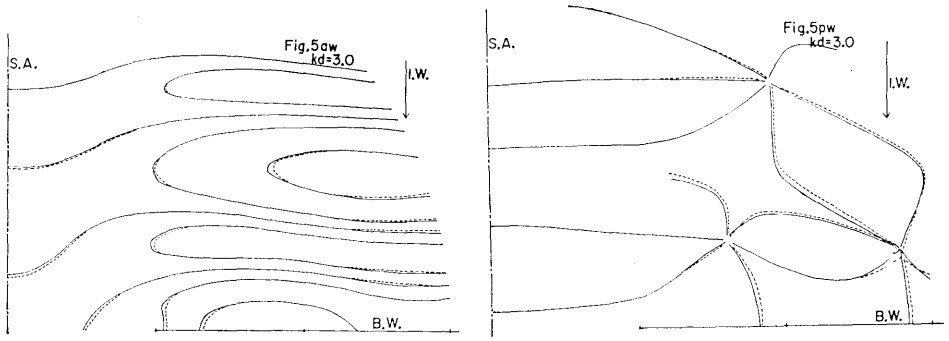

Fig. 5aw (pw). Comparison of the amplitudes (phases) in the windward based on the rigorous and mirror image method.*

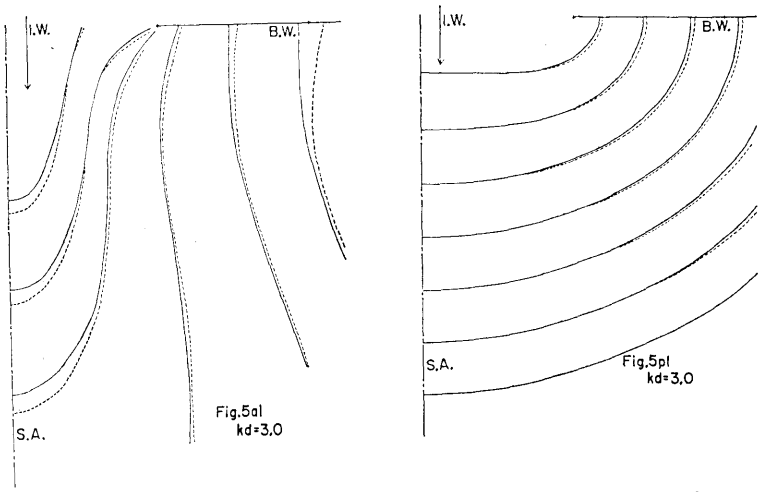

Fig. 5al (pl). Comparison of the amplitudes (phases) in the leeward based on the rigorous and mirror image method.*

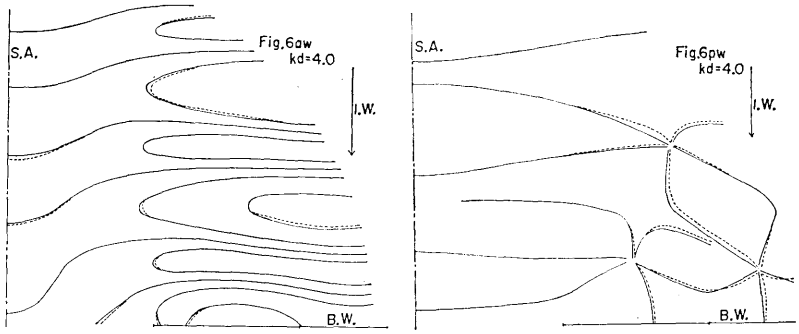

Fig. 6aw (pw). Comparison of the amplitudes (phases) in the windward based on the rigorous and mirror image method.*

* See the footnote of Figs. 2aw (pw)—3aw (pw).

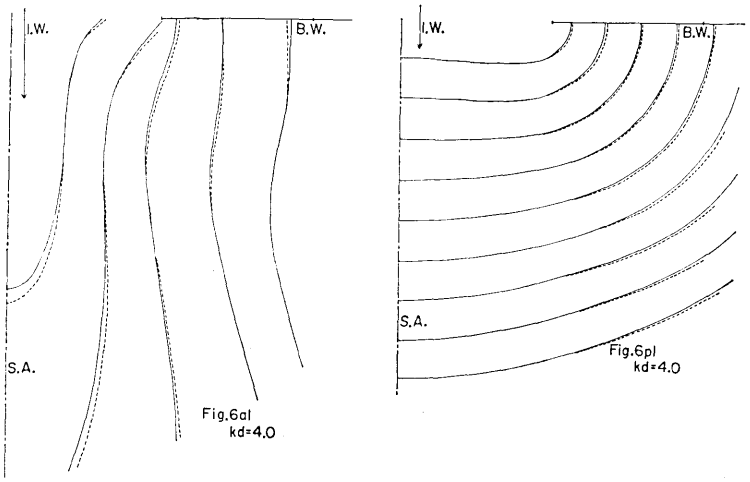

Fig. 6al (pl). Comparison of the amplitudes (phases) in the leeward based on the rigorous and mirror image method.*

which is Lamb's theory useful for the wave of $kd \lesssim 0.5$ and the other the theory of mirror image (which is completely the same as that devised by Blue-Johnson) capable of investigating the wave for $kd \gtrsim 0.5$.

3. Diffracted Wave

In this section, the diffracted wave from the left-hand breakwater is discussed, focussing the attention upon the effect of the right-hand breakwater on the above diffracted wave (refer to Fig. 7). For this purpose, the following procedure is devised.

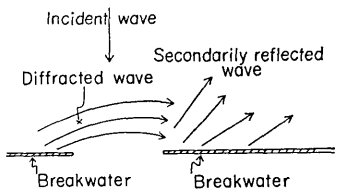

Fig. 7. Waves discussed.

Let $\zeta_{rigorous}$ and ζ_{single} be, respectively, the wave heights solved by the author and by Stoker, the former of which is given by ζ_j $(j=1, 2, 3)$ of (8) to (10) in the previous paper (*Momoi*, 1967a) and the latter by the first expression of (2). The gross effect ζ_{dif} of the right-hand breakwater upon the wave diffracted from the left one is then assessed by the equation

$$\zeta_{dif} = \bar{\zeta}_{rigorous} - \zeta_{single} \ , \qquad (3)$$

where $\bar{\zeta}_{rigorous}$ is a conjugate value of $\zeta_{rigorous}$ denoting the wave height for the incident wave $\exp(+i\omega t + iky)$ instead of $\exp(-i\omega t - iky)$. The above equation is illustrated in Fig. 8.

* See the footnote of Figs. 2aw (pw)—3aw (pw).

Using equation (3), the calculation is carried out for kd in the range 0.5 to 2.4. The computed results are presented in Figs. 9a (p) to 22a (p), where the suffixes a and p denote the figures relevant to the amplitude and phase.

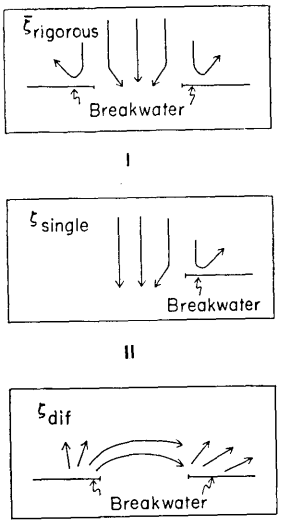

Fig. 8. Illustration of equation (3).

The variation of the amplitude is discussed in the beginning. Through Figs. 9a to 22a, the region of high amplitude is found along the right-hand breakwater in a shape varying with kd. The above region is located in the part slightly apart from the terminus of the breakwater for small kd (see Figs. 9a to 16a) with a moving nature toward the terminus for the increase of kd (refer to Fig. 23). The cause of the appearance of the low amplitude in the surrounding area of the terminus of the breakwater for $kd \lesssim 1.0$ (refer to Fig. 23) might be the result of a *negative interference* of the diffracted wave arriving directly from the left-hand breakwater with the secondarily reflected wave from the shadow of the right-hand breakwater (the illustration is given in Fig. 24), where the term of *negative interference* is used in such a sense that two waves interfere with each other with the phase shift of about π. As for the moving nature of the high amplitude region toward the breakwater terminus, it goes with the decay of the secondarily reflected wave from the breakwater shadow for the increase of kd. For the above-mentioned secondarily reflected wave, the reference to the figures of phase variation is preferable.

According to Figs. 9p and 11p, the emission of the wave reflected secondarily from the shadow of the right-hand breakwater is found definitely for $kd \lesssim 0.7$ (Case (i) of Fig. 25). As kd increases further, the component of the wave flowing into the leeward waters continues growing gradually to produce a pattern of the co-existence of both phase lines, one of which has the advancing nature toward the leeward waters and the other the nature reflected to the windward. The above nature of phase is found in the figures of phase of $kd=0.8$ to 1.4, i.e., Figs. 13p to 18p. The illustration for this case is given in Case (ii) of Fig. 25. As kd goes over 1.6, the reflected wave from the shadow of the breakwater is so weak that only the phase lines implying the inflow of the wave into the leeward are found in Figs. 19p to 22p. The illustration is given in Case (iii) of Fig. 25.

In the third work (*Momoi*, 1968a), we have discussed the appearance

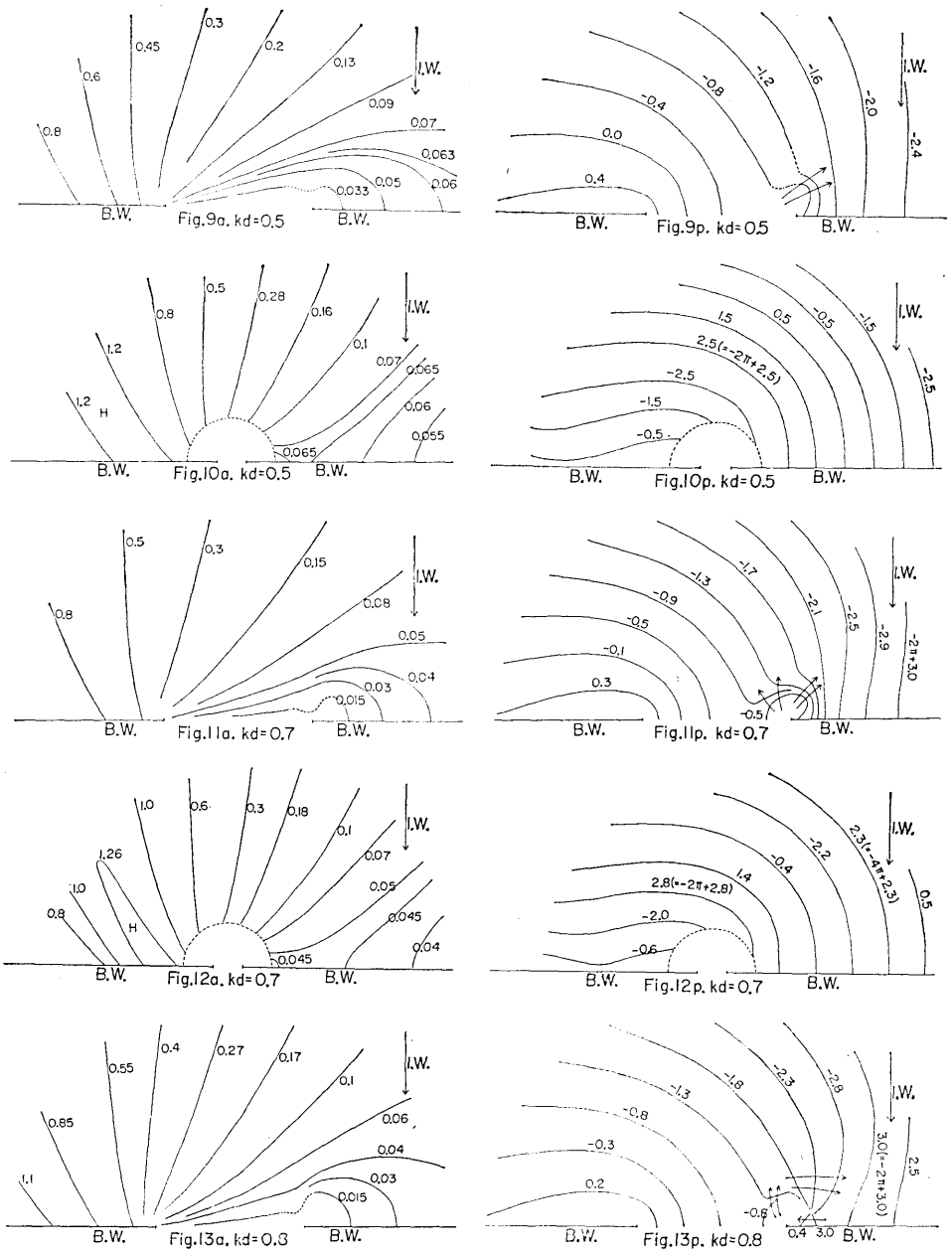

Figs. 9a (p)—13a (p). Amplitude (Phase) variation of the wave diffracted from the left-hand breakwater.**

** The left-hand and right-hand figures are respectively relevant to the amplitude and phase. **I. W.** and **B. W.** are the abbreviations of incident wave and breakwater. The numerals stated in the figures of the amplitude and phase denote $|\zeta_{dif}|$ and $\arg \zeta_{dif}$ respectively.

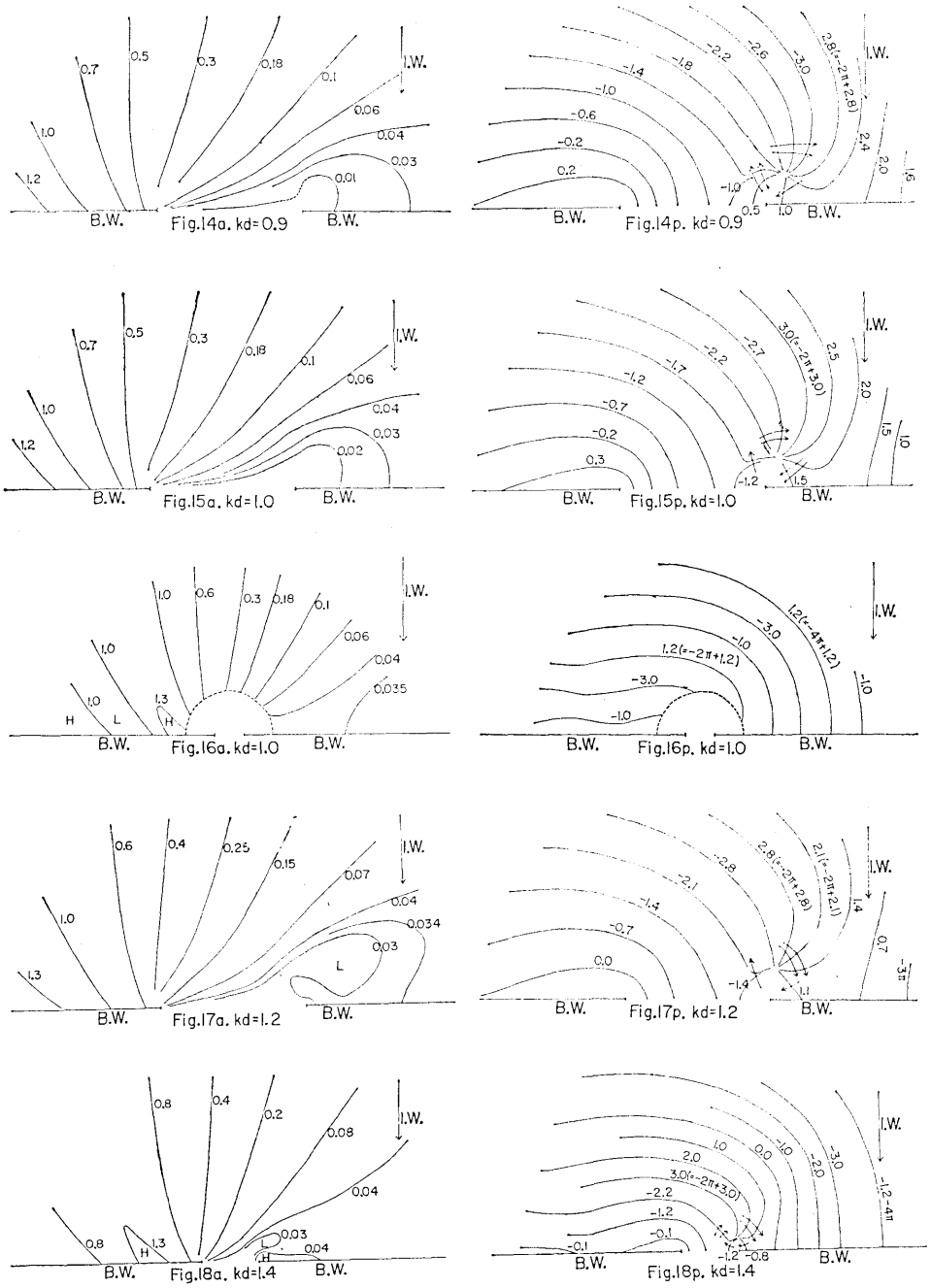

Figs. 14a (p)—18a (p). Amplitude (Phase) variation of the wave diffracted from the left-hand breakwater.**

** See the footnote of Figs. 9a (p)—13a (p).

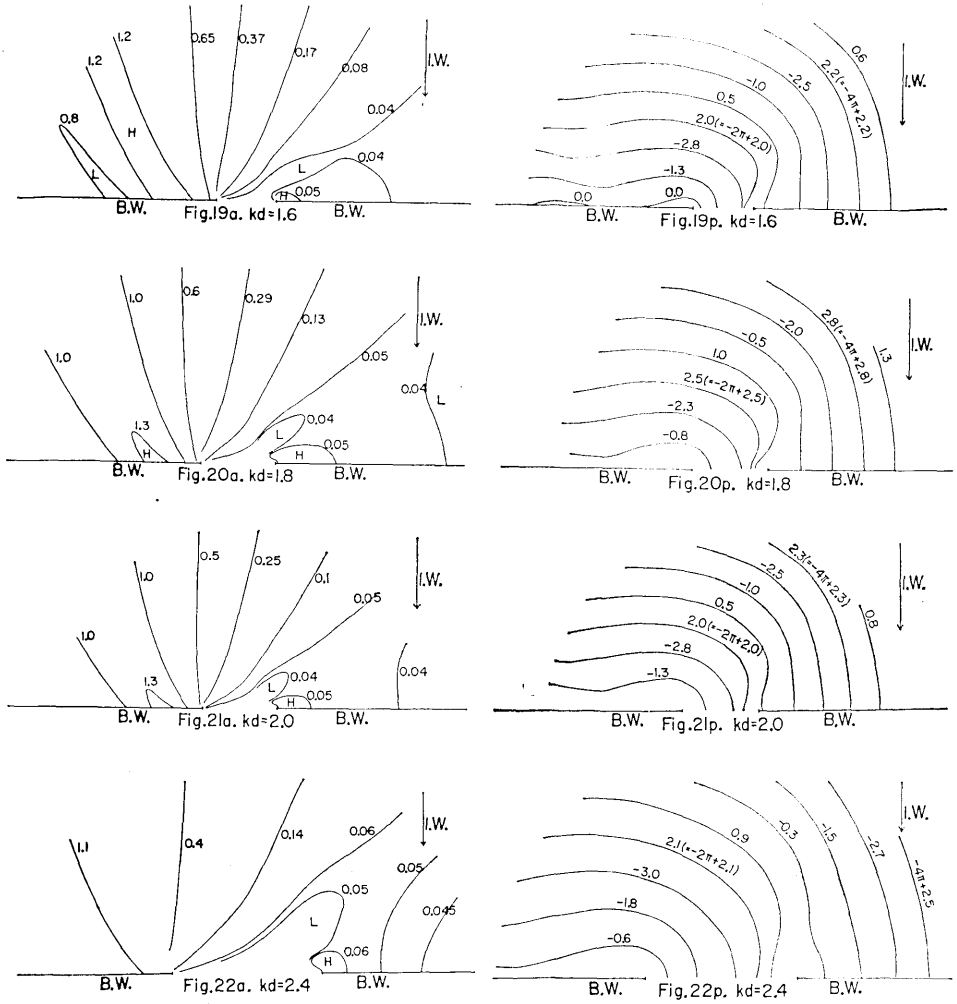

Figs. 19a (p)—22a (p). Amplitude (Phase) variation of the wave diffracted from the left-hand breakwater.**

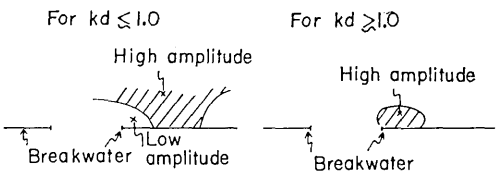

Fig. 23. Moving nature of high amplitude.

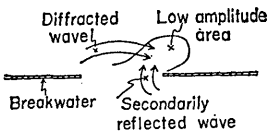

Fig. 24. Generation mechanism of low-amplitude area around the terminus of the right-hand breakwater for $kd \lesssim 10$.

** See the footnote of Figs. 9a (p)—13a (p).

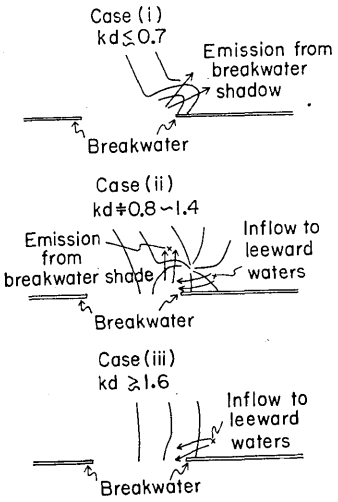

Fig. 25. Physical interpretation of the behavior of the phase line varying with the change of *kd*.

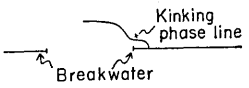

Fig. 26. Appearance of the kinking phase line for small *kd*.

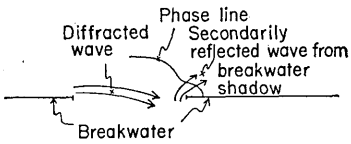

Fig. 27. One of the possible causes for the generation of the kinking crest line.

of the kinking crest line near the terminus of the breakwater for the wave of $kd \lesssim 1.0$ (refer to Fig. 26). The physical interpretation was then given that the waves advancing towards the entrance near the terminus of the breakwater wing are retarded as the result of the collision of the waves with nearby part of the terminus of the breakwater. If the above interpretation is accepted, the same phenomenon might have to occur around the terminus of a single breakwater wing. As will be found in the later section, such a phenomenon is, however, not found around the single breakwater terminus. The interpretation made in the previous work is, therefore, not considered to be consistent with the above fact. Other causes must be sought for the explanation of the appearance of the kinking crest line. As one of the possible causes, the secondarily reflected wave from the shadow of the breakwater might be proposed, which is generated by the arrival of the diffracted wave from the other breakwater (the left-hand one in the present section) at the (right-hand) breakwater (refer to Fig. 27).

4. Secondary Reflection

The waves arriving at the sea-wall near the gap are, in part, diffracted toward the entrance to cause the secondary reflection around the breakwater terminus on the other side. In order to examine the secondary reflection around the breakwater gap, the following equation is proposed.

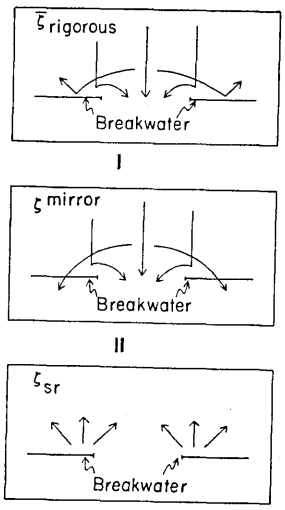

Fig. 28. Illustration of equation (4).

$$\zeta_{sr}=\bar{\zeta}_{rigorous}-\zeta^{mirror} \qquad (4)$$

where ζ_{sr} is the wave height denoting the secondary reflection around the gap, $\bar{\zeta}_{rigorous}$ and ζ^{mirror} those described in (3) and (1) respectively. The illustration of equation (4) is given in Fig. 28. As shown in the second picture of Fig. 28, the rigid breakwater for the incident wave behaves like a cushion-type breakwater for the diffracted wave (from the other sea-wall) based on the method of mirror image, in which no wave is secondarily reflected. Subtraction of the solution based on the method of mirror image from the rigorous one thus makes possible the evaluation of the secondary reflection around the breakwater gap.

Using equation (4), the calculation of the secondary reflection is made, the result of which is shown in Figs. 29a to 45a for the amplitude and in Figs. 29p to 43p for the phase.

According to the figures of the amplitude variation for $kd\lesssim 0.9$ (Figs. 29a to 35a), a pattern of multiply reflected waves, though so slight in intensity, is found around the gap (refer to Fig. 46). This behavior is not found in the figure relevant to the diffracted wave (Section 3) as the result of the suppression of the insignificant amount of the multiply reflected component by the overwhelming diffracted wave.

The same behavior as that of the diffracted wave is found in the figures of the secondary wave. That is to say, the region of high amplitude appears at the part slightly away from the terminus of the breakwater for small $kd\lesssim 1.0$ (Figs. 29a to 37a) with a low amplitude area around the terminus. The cause of this phenomenon might be considered to be a negative interference of the arriving wave diffracted from the other (left-hand) breakwater with the secondary wave reflected from the shadow of the (right-hand) breakwater. For the secondarily reflected wave described above, the emission from the breakwater shadow is also supported by the figure relevant to the phase variation. Referring to Fig. 29p, the phase line near the breakwater terminus runs clearly in a shape showing the emission of the wave from the breakwater shadow. The illustration is given in Fig. 47. As kd increases, the above secondary wave continues decreasing in intensity (refer to Figs. 33p to 38p) finally to be suppressed by the secondary wave reflected along the sea-wall facing the windward which is produced by the arrival of the diffracted

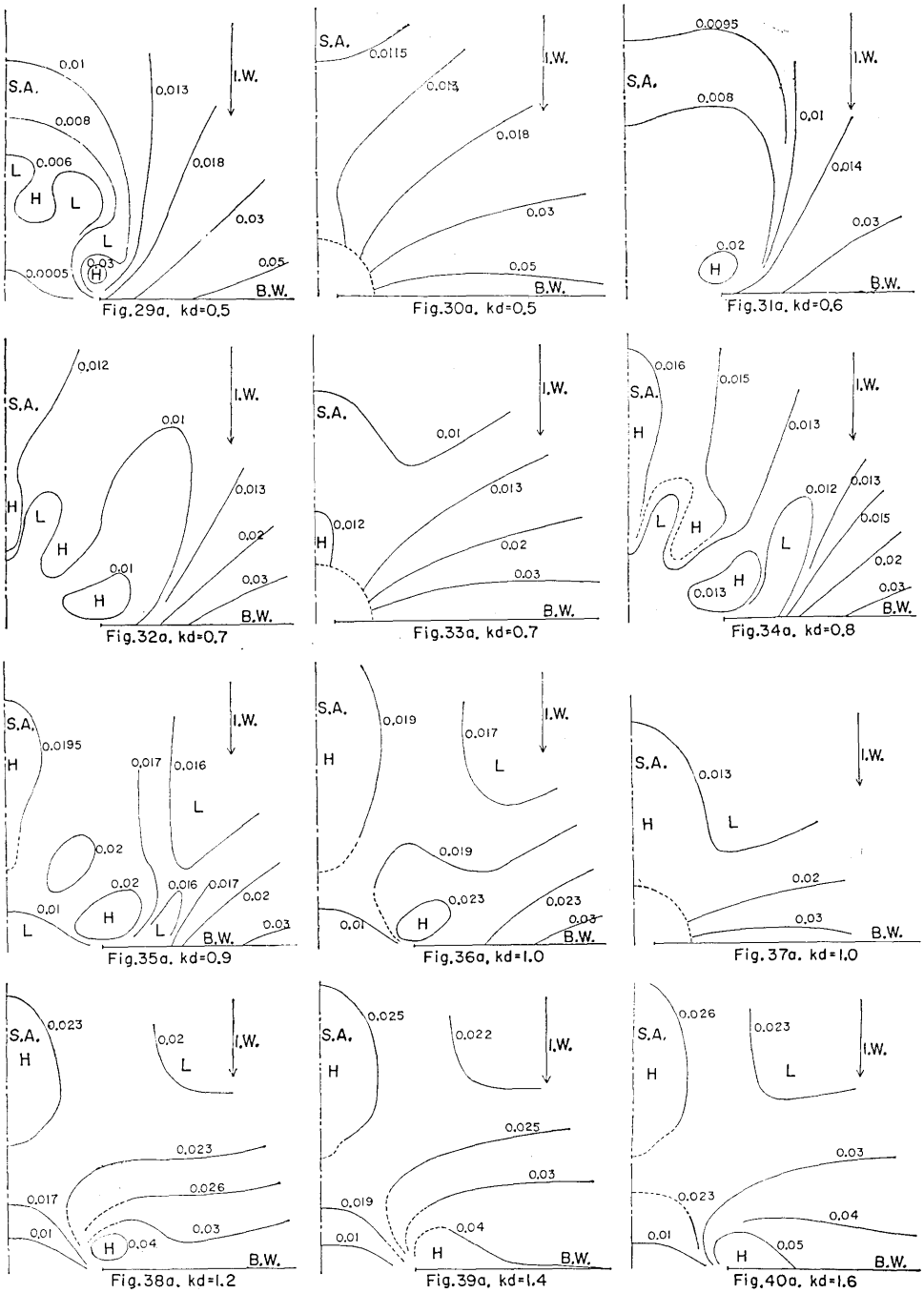

Figs. 29a—40a. Variation of the amplitude of the wave reflected secondarily from the breakwater wings.***

*** **I. W., S. A.** and **B. W.** are respectively the abbreviations of incident wave, symmetrical axis and breakwater. The values stated in the figures denote $|\zeta_{sr}|$.

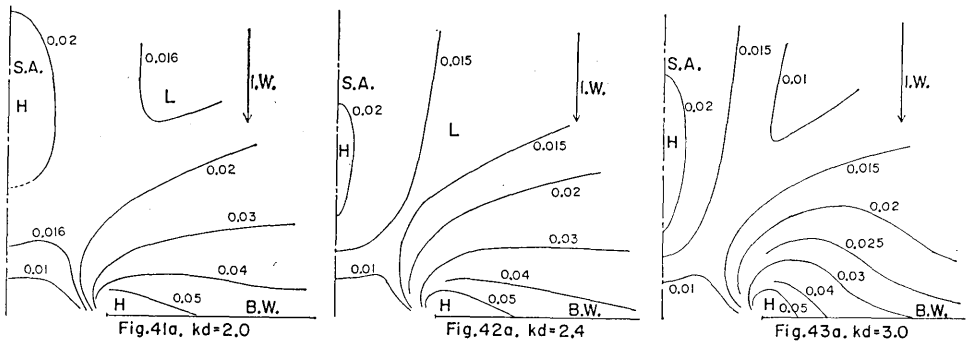

Fig.41a. kd=2.0 Fig.42a. kd=2.4 Fig.43a. kd=3.0

Fig.44a. kd=3.4 Fig.45a. kd=4.0

Figs. 41a—45a. Variation of the amplitude of the wave reflected secondarily from the breakwater wings.***

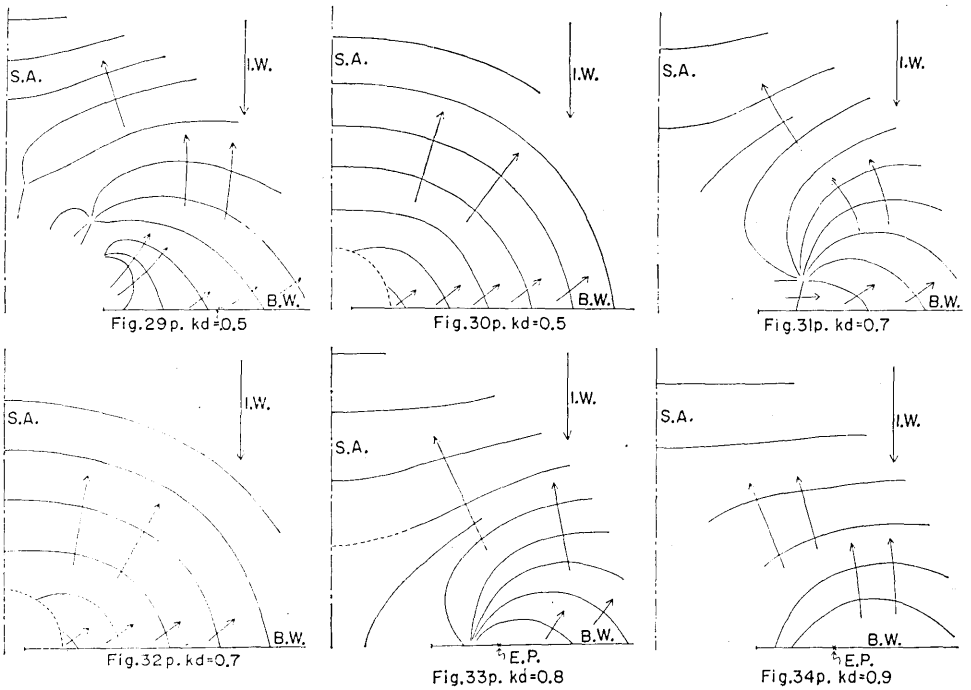

Fig.29p. kd=0.5 Fig.30p. kd=0.5 Fig.31p. kd=0.7

Fig.32p. kd=0.7 Fig.33p. kd=0.8 Fig.34p. kd=0.9

Figs. 29p—34p. Variation of the phase of the wave reflected secondarily from the breakwater wings.***

*** See the footnote of Figs. 29a—40a.

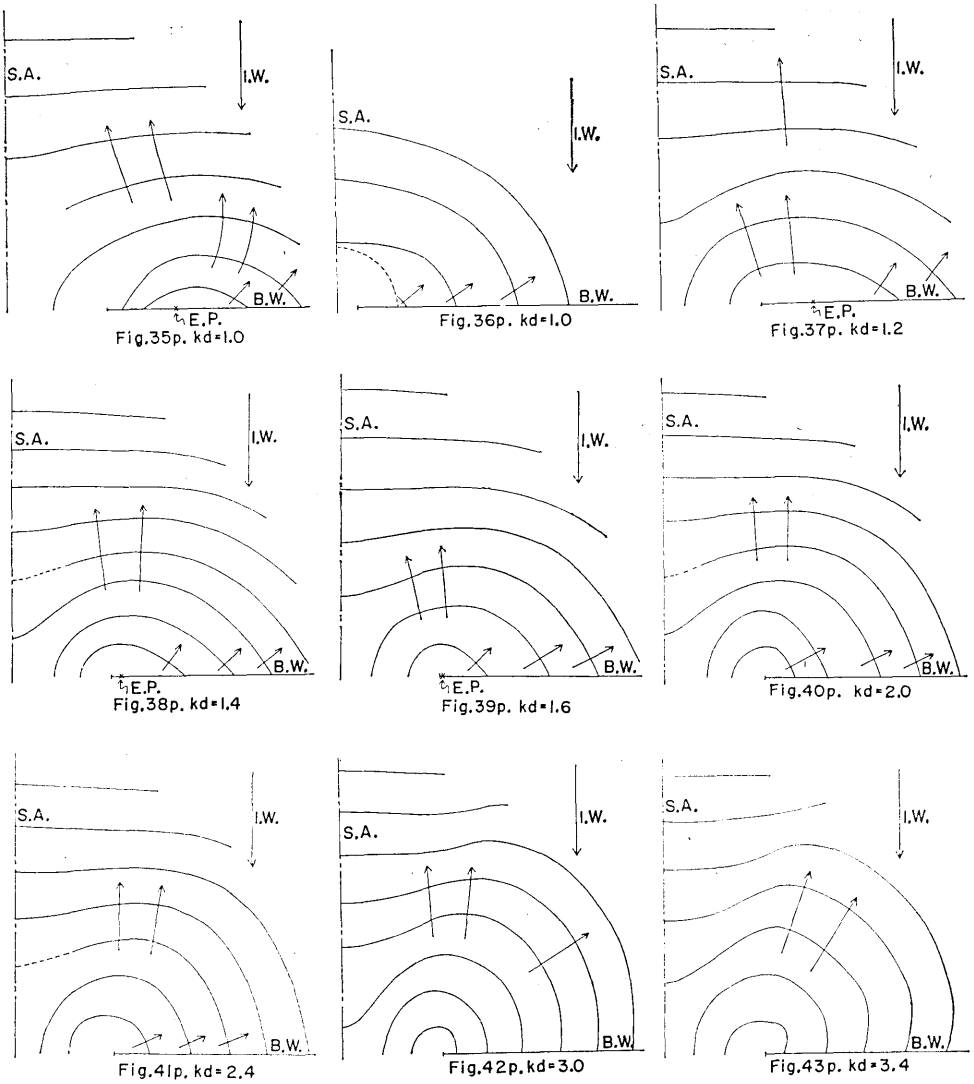

Figs. 35p—43p. Variation of the phase of the wave reflected secondarily from the breakwater wings.***

wave from the other breakwater. This tendency is also supported by two movements, one of which is the movement of the part of high amplitude toward the breakwater terminus with the increase of *kd* (see the figures of the amplitude) and the other that of the emitting point (shown by E. P. in Figs. 33p to 39p) of the wave. As for the

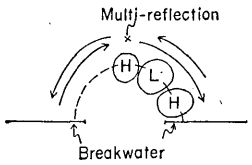

Fig. 46. Appearance of multiply reflected wave around the gap.

*** See the footnote of Figs. 29a—40a.

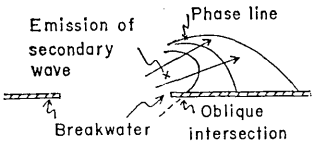

Fig. 47. Illustration of the emission of the secondary wave from the breakwater shadow. The crest line runs in a circular form, intersecting obliquely with the breakwater wing which shows definitely the emitting nature of the wave from the breakwater shadow.

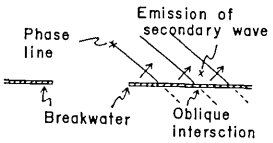

Fig. 48. Emission of the secondary wave at the breakwater on the windward side.

secondary reflection at the breakwater on the windward side, the oblique intersection of the phase line with the breakwater wing denote the emission of the secondary wave (refer to Fig. 48).

5. Wave around a Single Breakwater

In this section, the wave around the single breakwater wing for the case of the normal incidence of the incident wave is discussed with a view to inquring to what extent the behavoir of the wave around the twin breakwater wings comes from the coupling effect of the two breakwaters. The calculation is based on Stoker's result (*Stoker*, 1957), which is given by (1) of the sixth paper (*Momoi*, 1969) with $\alpha=\pi/2$. The definition and notation used in the present paper are then exactly the same as those of the previous paper. The calculated results are shown in Figs. 49a (p) to 52a (p) for the RST (resultant) wave and in Figs. 53a (p) to 56a (p) for the RD (reflected and diffracted) wave. The RST wave expressed by (1) of the sixth paper (*Momoi*, 1969), the RD wave being the purely reflected and diffracted one exclusive of the incident wave from the RST wave.

According to Figs. 49a to 52a, the regions of high amplitude (the shaded regions in the figures) are found along and in the frontal area of the breakwater on the windward side, the feature of which has been also found in the case of the twin breakwaters (refer to the second work (*Momoi*, 1967b)). The generation mechanism of the above high-amplitude regions is such that the high-amplitude part near the breakwater terminus is the result of the collision of the diverted wave appearing near the terminus with the sea-wall. The presence of the lastly stated diverted wave is ascertained from the figure of the phase (see the arrow of Fig. 51p). As for the high-amplitude regions off-shore, they are produced by the interference of a packet of the wave reflected obliquely from the part of the breakwater near the terminus (see Figs. 56a (p)) with the wave reflected normally from the breakwater.

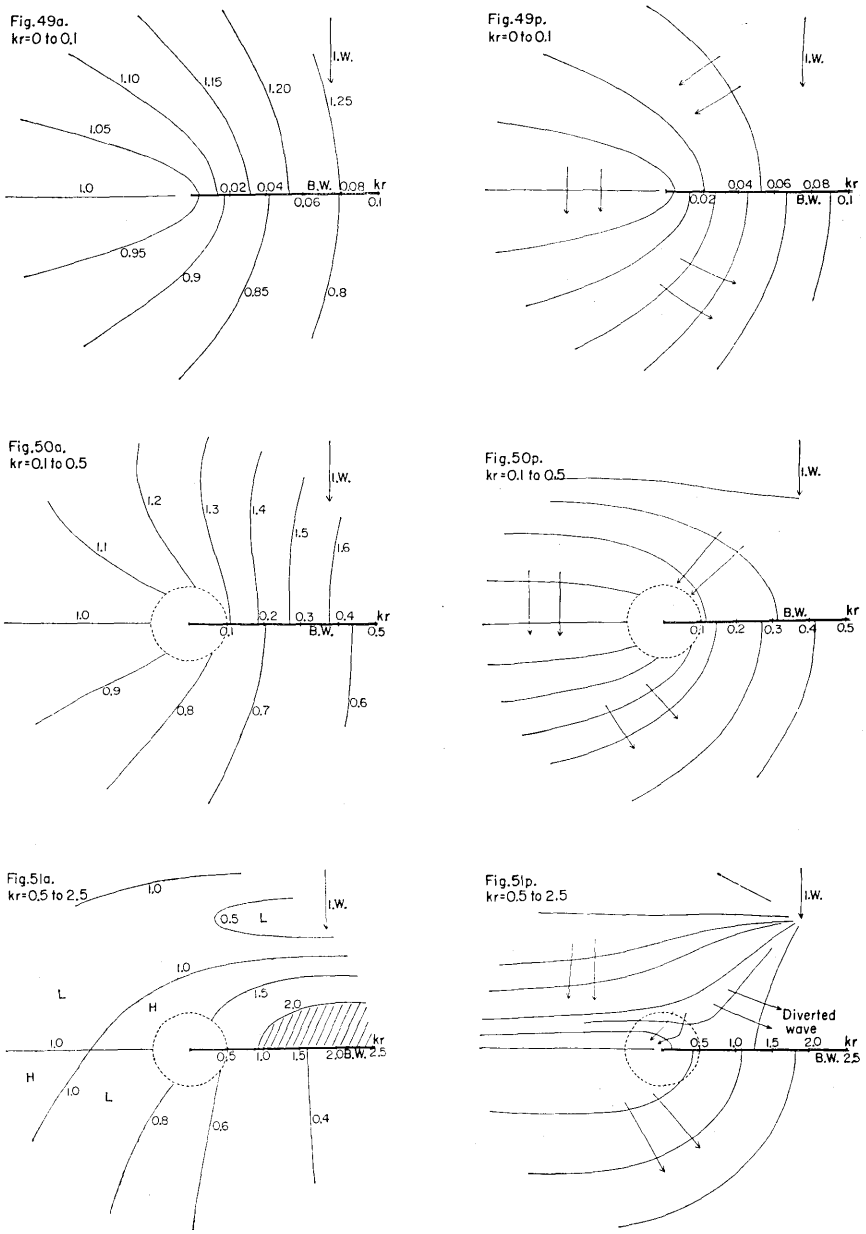

Fig. 49a (p)—51a (p). Variation of the amplitude (phase) of RST wave around the single breakwater wing.†

† **I. W.** and **B. W.** denote incident wave and breakwater. The subscript a and p stand for the figures relevant to the amplitude and phase. The values stated at the curves in the figures of the amplitude are $|\zeta_{single}|$. The curves of the phase are drawn on the basis of $\arg \zeta_{single}$.

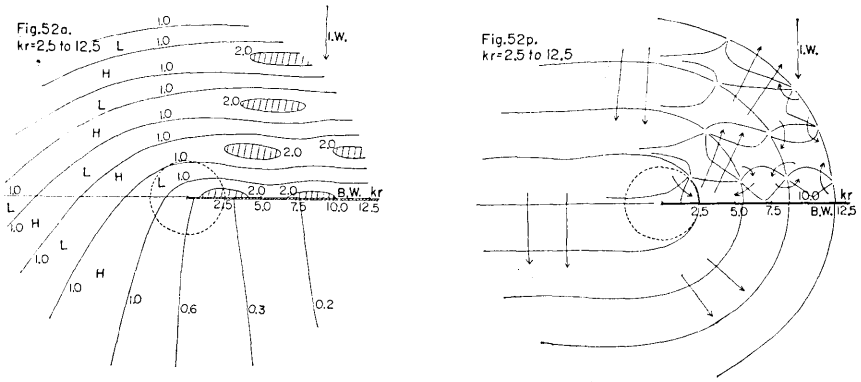

Figs. 52a and 52p. Variation of the amplitude and phase of RST wave around the single breakwater wing.†

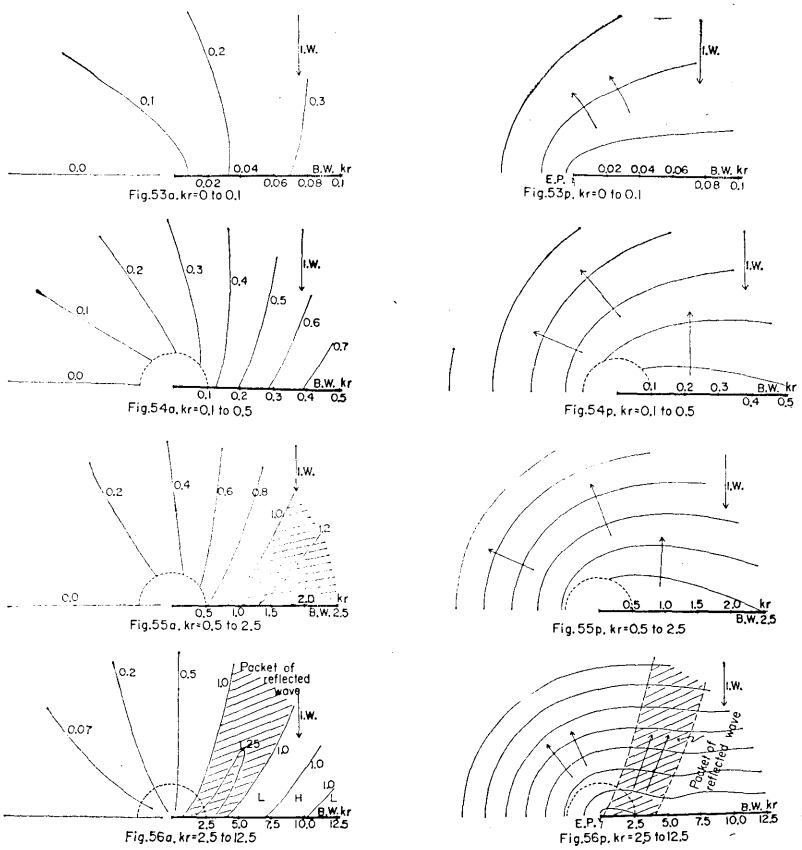

Figs. 53a (p)—56a (p). Variation of the amplitude (phase) of RD wave around the single breakwater wing.† The values stated at the curves of the amplitude are $|\zeta_{rd}|$, where $\zeta_{rd}=\zeta_{single}-\exp(iky)$. The curves of the phase are drawn on the basis of $\arg\zeta_{rd}$.

† See the footnote of the previous page.

The former is the reflection of the afore-mentioned diverted wave and the latter the normal reflection of the incident wave at the breakwater. The illustration is given in Fig. 57. These phenomena are also exposed in the analysis of the wave around the breakwater gap. The similar phenomena pertinent to the double breakwater wings are, therefore, not due to the coupling effect of the two breakwater wings, but the behaviors proper to the single breakwater wing.

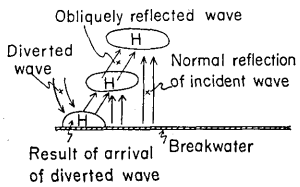

Fig. 57. Illustration of the generation mechanism of the high-amplitude areas. **H** is the abbreviation of high amplitude.

In the third work (*Momoi*, 1968a) concerning the wave around the breakwater gap, the kinking phase lines have been found in the nearby waters of the breakwater terminus. On inspection of Figs 49p to 52p, such kinking lines are not found in these figures. As discussed in Section 3, the cause of the above kinking phase lines might be ascribed to the coupling effect of the two breakwater wings.

References

Blue, F. L. Jr. and J. W. Johnson, 1949, Diffraction of Water Waves Passing through a Breakwater Gap, *Trans. Amer. Geophys. Union*, **30**, 705-718.

Momoi, T., 1967a, 1967b, 1968a, 1968b, 1968c and 1969, A Long Wave around a Breakwater [I], [II], [III], [IV], [V] and [VI], *Bull. Earthq. Res. Inst.*, **45**, **45**, **46**, **46**, **46** and **47**, 91-136, 749-783, 125-135, 319-343, 889-899 and 165-184.

Stoker, J. J., 1957, Water Waves, *Interscience Publishers, Inc., New York*, 109-133.

---

30. 防波堤のまわりにおける長波 [VII]

地震研究所 桃 井 高 夫

本報告においては，前報告に引きつづいて間隙をもつた防波堤のまわりにおける長波が論じられている．論ぜらている問題は次のごとくである．(1) *Blue-Johnson* の理論と筆者の厳密解との一致性，(2) 回折波に対する防波堤の効果，(3) 2 次的な反射波，および (4) 単一防波堤のまわりの長波の解析を通して，間隙をもつた防波堤のまわりの長波がどの程度二つの防波堤の相互作用にともづいているかを調べている．